CrystEngComm

Journal Name

ARTICLE

Synthesis, structures and luminescent properties of lanthanide coordination polymers involving biphenyl-3, 4', 5 -tricarboxylate

Xiang-Ying Li, [a,b] Zu-Jin Lin, [a] Yan-Yan Yang, [a,c] and Rong Cao*[a]

Based on biphenyl -3, 4', 5-tricarboxylate (H_3BPT), a series of lanthanide coordination polymers (CPs) formulated as $\{[Ln_2(BPT)_2(DMF)(H_2O)_3]\cdot 2DMF\cdot 3H_2O\}_n$ [Ln = Ce (**1**), Pr (**2**) and Eu (**3**); DMF = N, N-dimethylformamide], $\{[Ln_2(BPT)_2(DMA)_2(H_2O)_3]\cdot 0.5DMA\cdot 2.5H_2O\}_n$ [Ln = La (**4**), Sm (**5**), Eu (**6**) and Tb (**7**); DMA = N, N-dimethylacetamide] and $\{[Ln(BPT)(DMSO)_2]\cdot H_2O\}_n$ [Ln = Sm (**8**) and Nd (**9**); DMSO = dimethyl sulfoxide] have been synthesized and characterized. Compounds **1-3** are isostructural, and all of them exhibit three-dimensional networks with one-dimensional (1D) pear-shaped channels along the crystallographic a-axis and 1D rectangular channels along the crystallographic c-axis filled with free and coordinated solvents. Compounds **4**-**7** are isostructural, and each of the frameworks displays a 3D network exhibiting 1D channels filled with free and coordinated solvent molecules. Compounds **8**-**9** are isostructural and their structures are similar to that of **1**-**3** except for the different lanthanide ions and coordinated solvents. Structure analysis reveals that the net of **1**-**3** and **8**-**9** is a 3, 6-connected net with point symbol of $(4^2\cdot 6)^2(4^4\cdot 6^2\cdot 8^7\cdot 10^2)$, a subnet of **flu** net, while the net of **4**-**7** is a 3, 3, 6, 6-connected net with point symbol of $(4\cdot 6^2)^2(4^2\cdot 6^6\cdot 8^5\cdot 10^2)(4^2\cdot 6^2)(4^4\cdot 6^5\cdot 8^5\cdot 10)$. Luminescent measurements showed that compounds **3**, **6**, **7**, and **9** exhibit the characteristic emission bands for corresponding Ln(III) ions, while the emission spectra of **5** and **8** are mainly dominated by the ligand-based emission.

Introduction

Coordination polymers (CPs) have received considerable attention because of their intriguing topologies[1] and potential applications in gas storage and separation[2], catalysis,[3] luminescence,[4] proton conduction etc.[5] So far, large quantities of coordination polymers based on the fist-row transition metal ions have been reported because the transition-metal ions could offer several readily exploitable secondary building units (SBUs) in the construction of CPs during the self-assemble process, which are essential for the rational design and control the framework of targeting CPs.[6] In contrast with the prolific production of CPs based on transition metal ions, the CPs based on lanthanide ions have received unparallel attention[7]. Compared to the first-row transition metal ions, lanthanide ions have larger coordination spheres and more flexible coordination geometries. Although sacrificing a measure of control, these characters make it a unique approach to discover of novel and unusual frameworks.[8] Furthermore, due to the unique optical properties arising from $4f$ electrons, lanthanide coordination polymers are potentially applicable for sensors, lighting devices, and optical storage.

The luminescent properties of lanthanide CPs have attracted intense attention since the report of β-diketonate complexes containing europium.[9] Generally, the luminescent properties of lanthanide CPs relay strong on the inorganic and organic components, and also the types of interactions between them. On one hand, the f electrons in lanthanide ions remain highly localized, and thus the emission behavior of lanthanide ions on the basis of f–f transitions have narrow wavelength ranges. On the other hand, the f-f electronic transitions are forbidden by parity (Laporte) selection rules, leading to weak absorbance and low quantum yields. Since the weak absorbance of free lanthanide ions limits their luminescence intensity, lanthanide ions need to be sensitized by a suitable chromophoric moiety, which can be realized by judicious choice of chromophoric moieties serving as organic linkers within the realm of CPs. The use of polycarboxylic acids acting as chromophoric moieties is one of the common and efficient methods to construct lanthanide CPs with high luminescent quantum yields. For example, very recently, Liu and Zheng *et al.* employed 1,1',1''-(benzene-1,3,5-triyl)tripiperidine-4-carboxylic acid to prepare a series of lanthanide CPs (denoted as Ln-BTPCA in the original article).[10] With the adjustment of the relative concentration of the lanthanide ions, the color of the

luminescence can be modulated, and white light-emission with a quantum yield of 46.15% can be achieved. We and others have used H_3BPT to synthesize a series of lanthanide CPs with highly luminescent intensity.[11] In continuation of this theme, herein, nine 3D lanthanide CPs have further been constructed based on H_3BPT by altering the solvothermal reaction conditions. The resulting lanthanide CPs are 3D frameworks with channels filled with solvent molecules. Topology analysis showed that the net of **1-3** and **8-9** is a subnet of **flu**, while the net of **4-7** is a new topology with point symbol of $(4\cdot6^2)^2(4^2\cdot6^6\cdot8^5\cdot10^2)(4^2\cdot6^2)(4^4\cdot6^5\cdot8^5\cdot10)$. Besides, luminescent measurements showed that compounds **3**, **6**, **7**, and **9** exhibit the characteristic emission bands for corresponding Ln(III) ions, while the emission spectra of **5** and **8** are mainly dominated by the ligand-based emission.
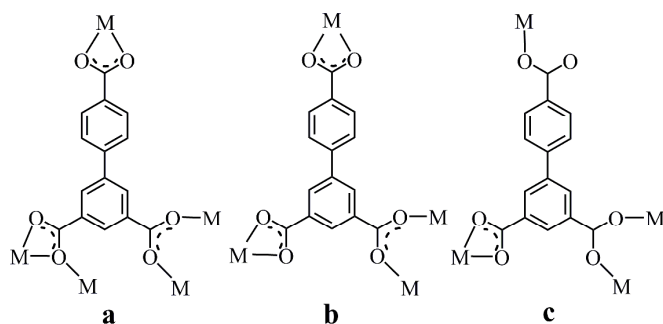
Scheme 1 Coordiantion modes of BPT^{3-} ligands.

Experimental Section

Materials and General Methods

All reagents were commercially available and used without further purification. Elemental analyses of C, H, N, and S were performed with a Vario MICRO EL Ⅲ elemental analyzer. Infrared (IR) spectra were recorded on PerkinElmer Spectrum instrument in the range of 4000-400cm^{-1} using KBr pellets. Thermogravimetric analyses (TGA) were performed on an SDT Q600 instrument under a nitrogen atmosphere with a heating rate of 10 ^{o}C min^{-1}. Powder X-ray diffraction (PXRD) patterns were recorded on a Rigaku Mini Flex Ⅱ diffractometer using Cu-Kα radiation (λ=1.54056Å) under ambient conditions. The solid-state photoluminescent spectra were measured on an Edinburgh FLS920 fluorescence spectrometer at room temperature. The instrument is equipped with an Edinburgh Xe900 xenon arc lamp as the exciting light source. In the testing process, all the excitation slits width was 3 nm wavelength resolution, the emission scan step was 0.2 nm, the emission scan dwell time was 0.1 s, and the focal length of the mono-chromator was 300 nm. The emission slits width of testing **3** was 0.25 nm wavelength resolution, while **6-8** were 0.3 nm, 0.5 nm and 0.13 nm, respectively. The data acquiring technique was single photon counting mode. For calculation method refer to the article published by de Mello *et al.*[12].

Synthesis of {[Ln$_2$(BPT)$_2$(DMF)(H$_2$O)$_3$]·2DMF·3H$_2$O}$_n$ [Ln = Ce (1), Pr (2), and Eu (3)]

A mixture of Ln(NO$_3$)$_3$·6H$_2$O [Ln = Ce (**1**), Pr (**2**), and Eu (**3**)] (0.06 mmol), H$_3$BPT (13.1 mg, 0.05 mmol) and NaOH (9.6 mg, 0.24 mmol) was dissolved in a mixed solvent of DMF (2 mL), ethanol (2 mL) and distilled water (2 mL). The mixture was ultrasonic stirred for 15 min and heated at 95 ℃ for 3 days, then cooled to room temperature.

For **1**: Colorless block-shaped large crystals were collected in 75% yield based on H$_3$BPT. Anal. Calcd for C$_{39}$H$_{47}$N$_3$O$_{21}$Ce$_2$ (%): N, 3.58; C, 39.90; H, 4.03. Found: N: 3.57; C, 37.88; H, 3.99. IR (KBr, cm^{-1}): 3420 (s), 1655 (w), 1618 (w), 1577 (w), 1537 (w), 1443 (w), 1408 (m), 1289 (w), 1257 (w), 1187 (w), 1107 (m), 1067 (w), 1016 (w), 925 (w), 869 (w), 849 (w), 779 (s), 723 (s), 670 (w), 540 (w), 466 (w).

For **2**: Light green block-shaped large crystals were collected in 70% yield based on H$_3$BPT. Anal. Calcd for C$_{39}$H$_{47}$N$_3$O$_{21}$Pr$_2$ (%): N, 3.57; C, 39.85 H, 4.03. Found: N: 3.31; C, 36.28; H, 3.91. IR (KBr, cm^{-1}): 3434 (s), 1662 (w), 1618 (w), 1578 (w), 1533 (w), 1442 (w), 1398 (s), 1289 (w), 1249 (w), 1184 (w), 1107 (m), 1063 (w), 1015 (w), 924 (w), 874 (w), 850 (w), 766 (s), 720 (s), 676 (w), 537 (w), 469 (w).

For **3**: Colorless block-shaped large crystals were collected in 75% yield based on H$_3$BPT. Anal. Calcd for C$_{39}$H$_{47}$N$_3$O$_{21}$Eu$_2$ (%): N, 3.51; C, 39.11; H, 3.96. Found: N: 3.40; C, 37.93; H, 4.17. IR (KBr, cm^{-1}): 3413 (s), 1620 (w), 1583 (w), 1542 (m), 1446 (w), 1397 (s), 1297 (w), 1262 (w), 1186 (w), 1113 (w), 1066 (w), 1021 (m), 976 (w), 924 (w), 867 (w), 777 (s), 728 (s), 594 (w), 547(w), 472(w).

Synthesis of {[Ln$_2$(BPT)$_2$(DMA)$_2$(H$_2$O)$_3$]·0.5DMA·2.5H$_2$O}$_n$ [Ln = La (4), Sm (5), Eu (6), and Tb (7)]

A mixture of Ln(NO$_3$)$_3$·6H$_2$O [Ln = La (**6**), Sm (**7**), Eu (**8**), and Tb (**9**)] (0.06 mmol) and H$_3$BPT (13.1 mg, 0.05 mmol) was dissolved in a mixed solvent of DMA (2 mL), ethanol (2 mL) and distilled water (2 mL). The mixture was ultrasonic stirred for 15 min and heated at 95 ℃ for 3 days, then cooled to room temperature.

For **4**: Colorless large block crystals were collected in 78% yield based on H$_3$BPT. Anal. Calcd for C$_{40}$H$_{47.5}$N$_{2.5}$O$_{20}$La$_2$ (%): N, 3.02; C, 41.38; H, 4.12. Found: N: 2.99; C, 41.45; H, 4.21. IR (KBr, cm^{-1}): 3420 (s), 1614 (s), 1580 (w), 1538 (s), 1449 (w), 1402 (s), 1297 (w), 1259 (w), 1189 (w), 1114 (w), 1072 (w), 1016 (m), 966 (w), 923 (w), 873 (m), 777 (s), 721 (s), 598 (m), 538 (w), 467 (w).

For **5**: Colorless large block crystals were collected in 80% yield based on H$_3$BPT. Anal. Calcd for C$_{40}$H$_{47.5}$N$_{2.5}$O$_{20}$Sm$_2$ (%): N, 2.96; C, 40.58; H, 4.04. Found: N: 2.92; C, 39.71; H, 4.18. IR (KBr, cm^{-1}): 3379 (s), 1610 (s), 1585 (w), 1534 (s), 1453 (w), 1403 (s), 1296 (w), 1265 (w), 1192 (w), 1111 (w), 1073 (w), 1015 (m), 961 (w), 923 (w), 866 (m), 778 (s), 719 (s), 597 (m), 550 (w), 476 (w).

For **6**: Colorless large block crystals were collected in 77% yield based on H$_3$BPT. Anal. Calcd for C$_{40}$H$_{47.5}$N$_{2.5}$O$_{20.5}$Eu$_2$ (%): N, 2.95; C, 40.47; H, 4.03. Found: N: 3.20; C, 40.68; H,

4.21. IR (KBr, cm^{-1}): 3401 (s), 1618 (s), 1585 (w), 1540 (s), 1450 (w), 1400 (s), 1294 (w), 1260 (w), 1195 (w), 1121 (w), 1067 (w), 1014 (m), 963 (w), 930 (w), 873 (m), 777 (s), 721 (s), 599 (m), 547 (w), 476 (w).

For **7**: Colorless large block crystals were collected in 77% yield based on H$_3$BPT. Anal. Calcd for C$_{40}$H$_{47.5}$N$_{2.5}$O$_{20.5}$Tb$_2$ (%): N, 2.92; C, 40.00; H, 3.99. Found: N: 2.77; C, 39.16; H, 4.14. IR (KBr, cm^{-1}): 3394 (s), 1605 (s), 1583 (w), 1536 (s), 1454 (w), 1392 (s), 1286 (w), 1259 (w), 1189 (w), 1120 (w), 1067 (w), 1015 (m), 962 (w), 928 (w), 870 (m), 772 (s), 721 (s), 595 (m), 548 (w), 466 (w).

Synthesis of {[Ln(BPT)(DMSO)$_2$]·H$_2$O}$_n$ [Ln = Sm (8) and Nd (9)]

A mixture of Ln(NO$_3$)$_3$·6H$_2$O [Ln = Sm (**10**), Nd (**11**)] (0.06 mmol) and H$_3$BPT (13.1 mg, 0.05 mmol) was dissolved in a mixed solvent of DMSO (5 mL), and distilled water (5 mL). The mixture was ultrasonic stirred for 15 min and heated at 85 ℃ for 3 days, then cooled to room temperature.

For **8**: Colorless large block crystals were collected in 65% yield based on H$_3$BPT. Anal. Calcd for C$_{19}$H$_{21}$S$_2$O$_9$Sm (%): C, 37.54; H, 3.48; S, 10.55. Found: C, 36.65; H, 3.50; S, 9.87. IR (KBr, cm^{-1}): 3448 (s), 1625 (m), 1584 (m), 1536 (m), 1451 (w), 1401 (s), 1368 (w), 1180 (w), 1110 (w), 1016 (w), 958 (w), 870 (w), 778 (s), 708 (s), 622 (w), 537 (w), 466 (w).

For **9**: Lavender large block crystals were collected in 56% yield based on H$_3$BPT. Anal. Calcd for C$_{19}$H$_{21}$S$_2$O$_9$Nd (%): C, 37.93; H, 3.52; S, 10.66. Found: C, 37.02; H, 3.49; S, 10.04. IR (KBr, cm^{-1}): 3445 (s), 1624 (m), 1579 (m), 1538 (m), 1449 (w), 1403 (s), 1367 (w), 1170 (w), 1108 (w), 1017 (s), 959 (m), 871 (w), 849 (w), 773 (s), 721 (s), 616 (w), 534 (w), 468 (w).

Single-Crystal X-ray Crystallography

Single-crystal X-ray diffraction data of compounds **1-3** and **8-9** were performed on Oxford XCalibur E CCD-based diffractometer equipped with graphite-monochromated Mo-Kα radiation (λ= 0.71073 Å) by ω-scan mode at room temperature. Single-crystal X-ray diffraction data of compounds **4-7** were performed on SuperNova CCD-based diffractometer equipped with graphite-monochromated Mo-Kα radiation by ω-scan at 100 K. All of the structures were solved by direct methods and refined by the full-matrix least-squares method on F^2 with the SHELXTL-97 program.[13] All non-hydrogen atoms except for some solvent molecules were refined with anisotropic thermal parameters. The positions of hydrogen atoms attached to carbon atoms and nitrogen atoms were positioned geometrically. Hydrogen atoms were not modelled on water ligands for compounds **1-7**. Attempts to locate and model the highly disordered solvent molecules in the pores of compounds **1-3** and **8-9** were unsuccessful. Therefore, the SQUEEZE routine of PLATON was used to remove the diffraction contribution from these solvents to produce a set of solvent free diffraction intensities.[14] A summary of crystallographic data and structure refinement is listed in Tables 1-2. Selected bond lengths and angles for **1-9** were listed in Tables S1-4 in the Supporting Information. CCDC 981948-981956 contain the

crystallographic data for this paper. These data can be obtained free of charge from the Cambridge Crystallographic Date Center via www.ccdc.cam.ac.uk.

Results and discussion

Description of the crystal structures

Single-crystal X-ray diffraction studies showed that compounds **1-3** are 3D frameworks, crystallizing in the monoclinic space group $C2/c$. Because they are isostructural, herein, only the structure of **1** will be described in detail as a representative. As shown in Fig. 1, the asymmetric unit of **1** contains one crystallographically independent cerium ions, one BPT^{3-} ligand, half coordinated DMF and one and half coordinated water molecule. The coordination mode of BPT^{3-} ligands is shown in Scheme 1a. The central cerium ion (Ce1) is coordinated by nine oxygen atoms with two (O5C, O6C) from a chelating carboxyl group, two (O3C, O4C) from a chelating/bridging carboxyl group, two (O1, O2A) from two independent bis(monodentate) bridging carboxyl groups, one (O7) from a coordinated water molecule and the remanding one (O8) from half coordinated DMF molecule and half coordinated water molecule. The coordination environment of the central Ce(III) ion, represented by coordination polyhedron, is a slightly distorted tricapped trigonal prismatic (Fig. S1). Two adjacent Ce(III) ions are connected by two chelating/bridging and two bis(monodentate) bridging carboxyl groups, forming binuclear [Ce$_2$(COO)$_6$(DMF)$_2$(H$_2$O)$_3$] building units. These binuclear building units are further cross-linked by BPT^{3-} ligands to form a 3D network with intersected channels. In this structure, the coordinated water molecules occupy the rectangular channels along the crystallographic c-axis (Fig. 2a), while the coordinated DMF molecules are filled in the small pear-shaped channels along the crystallographic a-axis (Fig. 2b). Considering the bimetal [Ce$_2$(COO)$_6$(DMF)$_2$(H$_2$O)$_3$] building
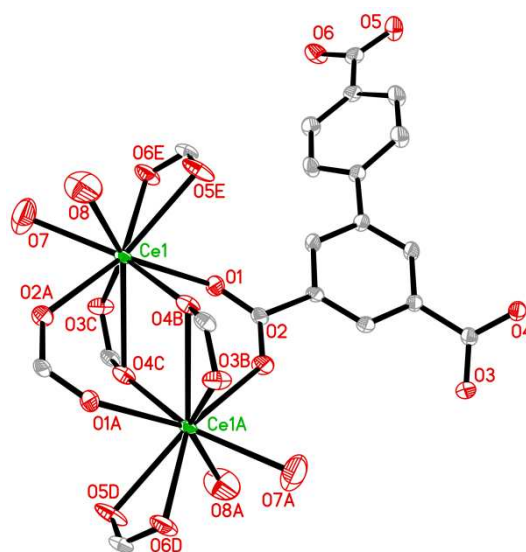
Fig. 1 The coordination environment of central Ce ion in **1**. The non-hydrogen atoms are represented by thermal ellipsoids drawn at the 30% probability level

(all H atoms, coordinated and free solvent molecules are omitted for clarity, O7 is from coordinated water and O8 is from half coordinated terminal DMF and half coordianted water). Symmetry transformations used to generate equivalent atoms: A, $-x + 1/2, -y + 3/2, -z$; B, $x, -y + 1, z + 1/2$; C, $-x + 1/2, y + 1/2, -z- 1/2$; D, $x - 1/2, -y + 3/2, z + 1/2$; E, $-x + 1, y, -z -1/2$

Table 1 Crystallographic data for **1-5**

	1	**2**	**3**	**4**	**5**
Chemical formula	$C_{39}H_{47}N_3O_{21}Ce_2$	$C_{39}H_{47}N_3O_{21}Pr_2$	$C_{39}H_{47}N_3O_{21}Eu_2$	$C_{40}H_{47.5}N_{2.5}O_{20}La_2$	$C_{40}H_{47.5}N_{2.5}O_{20}Sm_2$
Formula Mass	1174.04	1175.62	1197.72	1161.13	1184.01
Crystal system	Monoclinic	Monoclinic	Monoclinic	Monoclinic	Monoclinic
a/Å	24.8443(7)	24.7168(6)	24.5711(7)	20.2686(3)	19.8953(3)
b/Å	12.8836(4)	13.0121(4)	13.2963(4)	19.9736(2)	18.6848(2)
c/Å	15.0538(5)	14.9778(4)	14.7313(5)	27.9855(4)	27.9037(4)
α(°)	90.00	90.00	90.00	90.00	90.00
β(°)	96.709(3)	96.682(3)	96.735(3)	107.6320(10)	107.2660(10)
γ (°)	90.00	90.00	90.00	90.00	90.00
Unit cell volume/ Å^3	4785.5(3)	4784.4(2)	4779.6(3)	10256.7(2)	9905.48
T/K	293	293	293	100	100
Space group	C2/c	C2/c	C2/c	C2/c	C2/c
Z	4	4	4	8	8
μ/mm^{-1}	1.958	2.092	2.680	1.715	2.422
Data measured	13297	10032	24841	52229	46443
Unique data	5328	5144	5419	11283	10875
R_{int}	0.0315	0.0285	0.0721	0.0562	0.0425
R_1[a] $(I>2\sigma(I))$	0.0343	0.0344	0.0488	0.0819	0.0359
$wR(F^2)$[b] $(I>2\sigma(I))$	0.0962	0.0958	0.1320	0.2049	0.0850
R_1[a](all data)	0.0456	0.0484	0.0680	0.1005	0.0527
$wR(F^2)$[b] (all data)	0.1011	0.1019	0.1476	0.2214	0.0967
Goodness of fit on F^2	1.047	1.061	1.074	1.013	1.059
CCDC number	981948	981949	981950	981951	981952

[a] $R_1 = \sum||F_o| - |F_c||/\sum|F_o|$. [b] $wR_2 = \{\sum[w(F_o^2 - F_c^2)^2/\sum[wF_o^2]^2]\}^{1/2}$.

Table 2 Crystallographic data for **6-9**

	6	**7**	**8**	**9**
Chemical formula	$C_{40}H_{47.5}N_{2.5}O_{20}Eu_2$	$C_{40}H_{47.5}N_{2.5}O_{20}Tb_2$	$C_{19}H_{21}S_2O_9Sm$	$C_{19}H_{21}S_2O_9Nd$
Formula Mass	1187.23	1201.15	607.83	601.72
Crystal system	Monoclinic	Monoclinic	Monoclinic	Monoclinic
a/Å	19.8267(3)	19.7427(3)	24.8112(8)	24.8718(8)
b/Å	18.8685(2)	18.4330(2)	13.7461(4)	13.7591(4)
c/Å	27.9510(4)	27.8981(4)	13.6627(4)	13.6832(4)
α(°)	90.00	90.00	90.00	90.00
β(°)	107.1000(10)	107.3330(10)	99.153(3)	98.949(2)
γ (°)	90.00	90.00	90.00	90.00
Unit cell volume/ Å^3	9836.3(2)	9691.6(2)	4600.4(2)	4625.6(2)
T/K	100	100	293	293
Space group	C2/c	C2/c	C2/c	C2/c
Z	8	8	8	8
μ/mm^{-1}	2.602	2.971	2.780	2.471
Data measured	49468	46707	9536	8860
Unique data	10816	10637	4282	4316
R_{int}	0.0622	0.0626	0.0339	0.0258
R_1[a] $(I>2\sigma(I))$	0.0636	0.0609	0.0399	0.0379
$wR(F^2)$[b] $(I>2\sigma(I))$	0.1451	0.1564	0.1111	0.1085
R_1[a](all data)	0.0859	0.0754	0.0471	0.0446
$wR(F^2)$[b] (all data)	0.1611	0.1690	0.1162	0.1136
Goodness of fit on F^2	1.041	1.031	1.086	1.093
CCDC number	981953	981954	981955	981956

[a] $R_1 = \sum||F_o| - |F_c||/\sum|F_o|$. [b] $wR_2 = \{\sum[w(F_o^2 - F_c^2)^2/\sum[wF_o^2]^2]\}^{1/2}$.

Journal Name

ARTICLE

units as 6-connected nodes and the BPT^{3-} as 3-connected nodes, the structure of **1** can be viewed as a 3,6-connected net with point symbol of $(4^2 \cdot 6)^2 (4^4 \cdot 6^2 \cdot 8^7 \cdot 10^2)$, which is a subnet of **flu** net (Fig. 3a). The Ce-O bond lengths are in the range of 2.448-

Fig. 2 (a) The coordinated water molecules occupy in the rectangular channels along *c*-axis. (b) The DMF molecules are filled in the pear-shaped channels along the *a*-axis. Only two coordinated water and two coordinated DMF molecules were shown in space-filling model for clarify. Colour scheme: Ce polyhedra, green; C, gray; O, red; N, yellow.

compatible with values of other reported cerium-oxygen donor compounds.[15]

Compounds **4**-**7** are isostructural and crystallize in the monoclinic space group *C*2/*c*. As a representative example, only the crystal structure of **5** is depicted here in detail. As shown in Fig. S2, the asymmetric unit of **5** contains two crystallographically independent Sm(III) ions, two BPT^{3-}, two

2.761 Å, and the O-Ce-O angles are in the range of 48.92-151.44°. All the Ce-O distances and O-Ce-O angles are

coordinated DMA and three coordinated water molecules. The coordination modes of BPT^{3-} ligands were shown in Scheme 1b, c. In the structure, one of the crystallographically independent samarium ion (Sm1) is eight coordinated by a chelating carboxyl group (O1, O2), two bis(monodentate) bridging carboxyl groups (O13B, O14C), a monodentate carboxyl group (O7A), two water molecules (O3, O4), and a DMA molecule (O5); the other (Sm2) is nine coordinated by a chelating carboxyl group (O11E, O12E), two chelating/bridging carboxyl groups (O10, O15, O10D), two bis(monodentate) bridging carboxyl groups (O8, O9D), a DMA (O17) and a water molecule (O16). The coordination environments of the Sm1 and Sm2 ions, represented by coordination polyhedra, are slightly distorted bicapped and tricapped trigonal prismatic, respectively (Fig. S3a, b). The Sm1 and Sm2 ions connect to their inverse ones to form two binuclear building blocks $Sm_2(COO)_6(DMA)(H_2O)_2$ and $Sm_2(COO)_6(DMA)(H_2O)$, respectively. In such way, the two bicapped trigonal prismatic in the former binuclear building block are bridged by two bis(monodentate) bridging carboxyl groups and the two tricapped trigonal prismatic in the latter binuclear building block are united by sharing an edge (Fig. S3c, d). The two different binuclear building units are alternatively cross-linked by BPT^{3-} ligands to form a 3D network with 1D channel filled with solvent molecules (Fig. 4). In the case of **5**, the structure can be viewed as a 3,3,6,6-connected net with point symbol of $(4 \cdot 6^2)^2 (4^2 \cdot 6^6 \cdot 8^5 \cdot 10^2)(4^2 \cdot 6^2)(4^4 \cdot 6^5 \cdot 8^5 \cdot 10)$ by considering the BPT^{3-} as 3-connected nodes and the bimetal building units as 6-connected nodes (Fig. 3b).
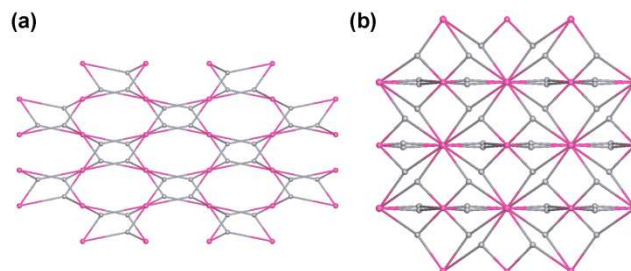
Fig. 3 (a) The topology of frameworks **1**-**3** and **8**-**9**. (b) The topology of frameworks **4**-**7**.
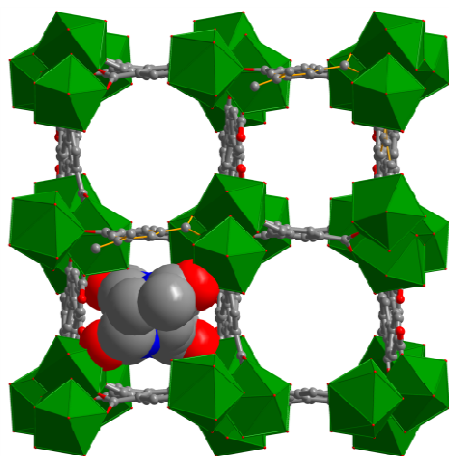
Fig. 4 Scheme shown 1D channels in **5** filled with solvent molecules. Only two coordinated DMF molecules were shown in space-filling model for clarify. Colour scheme: Sm polyhedra, green; C, gray; O, red; N, yellow.

Compounds **8-9** are isostructural and crystallize in the monoclinic space group *C*2/*c*. As a representative example, only the crystal structure of **8** is depicted. As shown in Fig. S4, the asymmetric unit of **8** contains a crystallographic Sm(III) ion, a BPT^{3-} ligand, two coordinated DMSO molecules. In this structure, the coordination mode of BPT^{3-} ligand (Scheme 1a), the coordination environments of the central ions, the binuclear building blocks and also the connection fashions are similar to that of **1**. Therefore, the skeleton of **8** is similar to that of **1** except for the different lanthanide ions and coordinate solvent molecules. Similar to **1**, compound **8** also has 1D pear-shaped channels along the crystallographic *a*-axis and 1D rectangular channels along the crystallographic *c*-axis, both of which are filled with coordinated DMSO molecules (Fig. S5). Topology analysis show that the topology of **8** is identical to that of **1**.

To check the purity and homogeneity of the bulk crystals of compounds **1-9**, the as-prepared samples of the nine compounds were measured by powder X-ray diffraction (PXRD) at room temperature. As shown Fig. S6-14 in the supporting information, the peak positions of the experimental patterns are in good agreement with the simulated ones, which clearly indicate the good purity and homogeneity of these samples. To investigate the thermal stability of compounds **1-9**, the thermogravimetric analyses were carried out on a SDT Q600 instrument in the temperature range of 30-900 ℃ under a flow of nitrogen with a heat rate of 10 ℃ min^{-1}. As shown in Fig. S15, compounds **1-3** show similar thermal stability due to the their isostructural nature of the framework. The continuous weight loss from room temperature to *ca*. 520 ℃ corresponds to the loss of all solvent molecules (calcd: 27.88 % for **1**, 27.83 % for **2**, and 27.32 % for **3**; found: 27.62 % for **1**, 28.71 % for **2**, and 28.82 % for **3**), which is followed by the framework collapse with increasing temperature. The thermal stability performed on compounds **4-7** is found that they also exhibit similar thermal stability (Fig. S16). For compound **4**, from room temperature to *ca*. 220 ℃, a total weight loss of *ca*. 7.93 % is attributed to the loss of free water and free DMA

molecules (calcd: 7.63 %). A total of 19.93 % is observed between 220 ℃ and 540 ℃, which is in agreement with the departure of coordianted water and DMA molecules (calcd: 19.66 %). The TG curves of compounds **5-7** are similar to that of **4**, where the first weight loss is 7.95 % for **5**, 7.33 % for **6**, and 7.67 % for **7** (calcd: 7.48 % for **5**, 7.46 % for **6**, and 7.37 % for **7**) from room temperature to 220 ℃. The second weight loss between 220 and *ca*. 540 ℃ is 21.27 % for **5**, 19.98 % for **6**, and 20.29 % for **7** (calcd: 19.28 % for **5**, 19.22 % for **6**, and 19.00 % for **7**). Likewise, because compounds **8-9** are isostructural, they show parallel thermal stability (Fig. S17). The first weight loss from room temperature to *ca*. 190 ℃ corresponds to the departure of a free water molecule (observed: 3.46 % for **8** and 3.29 % for **9**; calcd: 2.96 % for **8** and 2.99 % for **9**) and the second weight loss from 190 to *ca*. 540 ℃ is attribute to the loss of two coordinated DMSO molecules (observed: 26.82 % for **8** and 27.42 % for **9**; calcd: 25.70 % for **8** and 25.97 % for **9**). With the temperature reaching to 540 ℃, the framework starts to burn up.

Luminescent properties

Lanthanide coordination polymers are known for luminescent properties. The narrow, sharp and well-separated emission bands make them to serve as potential luminescent materials.[16] The organic linkers in coordination polymers could transfer the absorbed energy from light radiation to lanthanide ions *via* the antenna effect so as to obtain CPs with high luminescent quantum yields. To investigate the luminescent properties, the solid-state photoluminescent properties of compounds **3**, and **5-9** were measured on an Edinburgh FLS920 fluorescence spectrometer at room temperature. When excited at 300 nm, the free H$_3$BPT ligand exhibits a broad emission band at *ca*. 370 nm, which is ascribed to the intraligand $\pi \rightarrow \pi^*$ transitions.[11a] Upon an excitation at 306 nm, compounds **3** and **6** show the characteristic emission bands of Eu^{3+} ions. As shown in Fig. 6, the solid-state luminescent emission spectra of **3** and **6** are similar. The strong emissions at 614 nm are attributed to $^5D_0 \rightarrow ^7F_2$ transitions, the medium emission bands at 591.5 nm and 698 nm are attributed to $^5D_0 \rightarrow ^7F_1$ and $^5D_0 \rightarrow ^7F_4$ transitions, respectively. The weak emission bands at 579.5 nm and 650 nm correspond to $^5D_0 \rightarrow ^7F_0$ and $^5D_0 \rightarrow ^7F_3$ transitions, respectively. The emission spectra of **3** and **6** are dominated by the band of $^5D_0 \rightarrow ^7F_2$ transitions, the intensity of which are much stronger than the intensity of $^5D_0 \rightarrow ^7F_1$ transitions, indicating that the Eu^{3+} ions adopt non-centrosymmetric coordination modes, in agreement with the crystal structural analyses of **3** and **6**. The absence of ligand-based emission at *ca*. 380 nm suggests efficient energy transformation from the BPT^{3-} ligands to the lanthanide centres, which is further confirmed by the moderate luminescent quantum yields (12.25% for **3** and 20.59% for **6**). As shown in Table 3, the photoluminescent lifetimes are 559.65 μs for **3** and 661.94 μs for **6**.
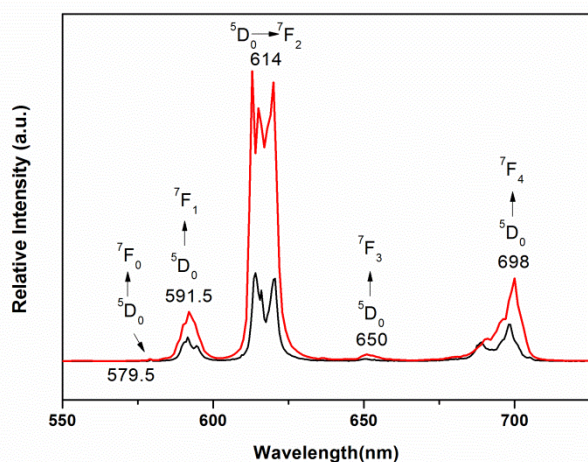
Fig. 6 The solid-state photoluminescent spectra of **3** (black) and **6** (red).

Table 3 The luminescent lifetimes and quantum yields of **3**, and **6-8**.

Compound	3^a	6^a	7^b	8^c
Lifetime (μs)	559.65	661.94	661.47	7.44
Quantum yield (%)	12.25	20.59	42.58	15.95

^{a} excited at 306 nm, ^{b} excited at 290 nm, ^{c} excited at 322 nm.
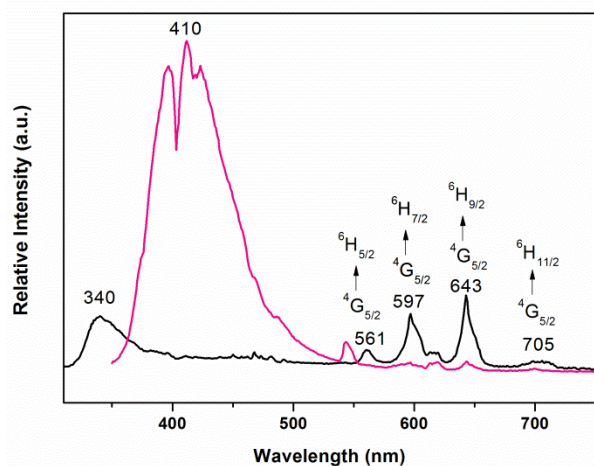
Fig. 7 The solid-state photoluminescent spectra of **5** (black)and **8** (pink).

As shown in Fig. 7, by comparison of the emission energies and profiles of the free H_3BPT ligand and compounds **5-8**, the luminescent emission spectra of **5** and **8** are dominated by ligand-based emission. The emission bands at *ca.* 340 nm for **5** and *ca.* 412 nm for **8** may be attributed to the ligand-based emission, which might be due to the intermolecular excimer-type interactions between ligands and ligand-to-ligand charge transitions (LLCT).[17]

Besides, compounds **5** and **8** display similar luminescent emissive spectra in the range of 500-750 nm for their same lanthanide ions (i.e., Sm^{3+}). The strong emission bands at 643 nm are related to $^4G_{5/2} \rightarrow {}^6H_{9/2}$ transitions, the medium emissions at 597 nm are related to $^4G_{5/2} \rightarrow {}^6H_{7/2}$, and the weak emissions at

561 nm and 705 nm are attributed to $^4G_{5/2} \rightarrow {}^6H_{5/2}$ and $^4G_{5/2} \rightarrow {}^6H_{5/2}$ respectively. The present of ligand-based emission suggests inefficient energy transfer from the BPT^{3-} ligands to the lanthanide centres. Compound **8** has a luminescent lifetime of 7.44 μs and a quantum yield of 15.95% (Table 3).
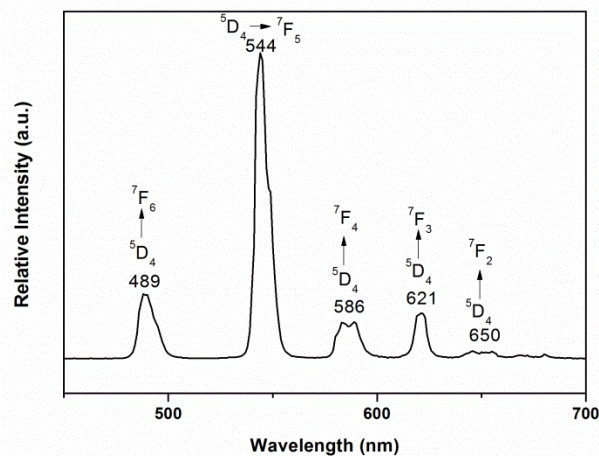
Fig. 8 The solid-state photoluminescent spectra of **7**.

Under an excitation of 290 nm, compound **7** shows the characteristic Tb^{3+} luminescent emission (Fig. 8). The strong emission band at 544 nm corresponds to the $^5D_4 \rightarrow {}^7F_5$ transition, and the medium emission bands at 489 nm, 586 nm and 621 nm are attributed to the $^5D_4 \rightarrow {}^7F_6$, $^5D_4 \rightarrow {}^7F_4$, and $^5D_4 \rightarrow {}^7F_3$ transitions, respectively. The weak peak at 650 nm arises from $^5D_4 \rightarrow {}^7F_2$ transition. Compound **7** has a luminescent lifetime of 661.47 μs. It is worth to note that the luminescent quantum yield of **7** is up to 42.58 %, albeit there are three coordinated water molecules and two coordinated DMF molecules in each asymmetric unit, which is usually believed to quench the lanthanide luminescence. However, the luminescent quantum yield is not so high for **6** even though **6** and **7** are isostructural. It is probably for the energy differences between the triplet position of H_3BPT ligand and the emissive energy levels of Ln^{3+} ions.[18]
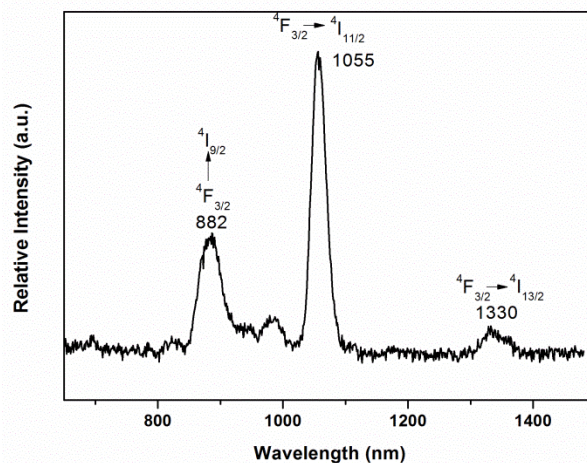
Fig. 9 The solid-state photoluminescent spectra of **9**.

As shown in Fig. 9, the profile of the emission bands in the range of 800-1500 nm for **9** are in agreement with previously reported spectra of Nd(III) complexes.[19] Under an excitation of 310 nm, compound **9** displays a strong emission at 1055 nm arising from $^4F_{3/2} \rightarrow {}^4I_{11/2}$ transition, a medium emission at 882 nm corresponding to $^4F_{3/2} \rightarrow {}^4I_{9/2}$ transition, and a weak emission at 1330 nm arising from $^4F_{3/2} \rightarrow {}^4I_{13/2}$ transition.

Conclusions

In conclusion, nine new 3D lanthanide coordination polymers, namely, $\{[Ln_2(BPT)_2(DMF)(H_2O)_3] \cdot 2DMF \cdot 3H_2O\}_n$ [Ln = Ce (**1**), Pr (**2**) and Eu (**3**)], $\{[Ln_2(BPT)_2(DMA)_2(H_2O)_3] \cdot 0.5DMA \cdot 2.5H_2O\}_n$ [Ln = La (**4**), Sm (**5**), Eu (**6**) and Tb (**7**)] and $\{[Ln(BPT)(DMSO)_2] \cdot H_2O\}_n$ [Ln = Sm (**8**) and Nd (**9**)] have been synthesized under solvothermal conditions based on H_3BPT. Compounds **1**-**3** are isostructural and all of them exhibit intersected channels filled with DMF and water molecules. Compounds **4**-**7** are isostructural, and all of them display 3D network exhibiting 1D channels filled with DMA and water molecules. Compounds **8**-**9** are isostructural and their structures are similar to that of **1**-**3** except for the coordinated solvent molecules. Luminescent measurements show that compounds **3**, **6**, **7**, and **9** exhibit the characteristic emission bands for corresponding Ln(III) ions, while the emission spectra of **5** and **8** are mainly dominated by the ligand-based emission. Remarkable, the luminescent quantum yield of **7** is up to 42.58 %.

Acknowledgements

Notes and references

[a] State Key Laboratory of Structural Chemistry, Fujian Institute of Research on the Structure of Matter, Chinese Academy of Sciences, Fujian, Fuzhou, 350002, P. R. China.
E-mail: rcao@fjirsm.ac.cn; Fax: (+86) 591-8379-6710; Tel: (+86) 591-8379-6710.
[b] University of the Chinese Academy of Sciences, Beijing, China.
[c] College of Chemistry and Chemical Engineering, Fuzhou University, Fuzhou, 350002, China.

Electronic Supplementary Information (ESI) available: X-ray crystallography, powder X-ray diffraction, thermogravimetric analysis, IR spectra, selected bonds and angles. See DOI: 10.1039/b000000x/

1 (a) N. Stock and S. Biswas, *Chem. Rev.*, 2012, **112**, 933; (b) G.-P. Yang, L. Hou, X.-J. Luan, B. Wu and Y.-Y. Wang, *Chem. Soc. Rev.*, 2012, **41**, 6992; (c) H.-L. Jiang, T. A. Makal and H.-C. Zhou, *Coord. Chem. Rev.*, 2013, **257**, 2232.

2 Z.-J. Lin, T.-F. Liu, Y.-B. Huang, J. Lü and R. Cao, *Chem.-Eur. J.*, 2012, **18**, 7896; (b) M. Du, C. P. Li, C. S. Liu and S. M. Fang, *Coord. Chem. Rev.*, 2013, **257**, 1282; (c) Z.-J. Lin, Y.-B. Huang, T.-F. Liu, X.-Y. Li and R. Cao, *Inorg. Chem.*, 2013, **52**, 3127.

3 S. Chaemchuen, N. A. Kabir, K. Zhou and F. Verpoort, *Chem. Soc. Rev.*, 2013, **42**, 9304.

4 (a) A. S. R. Chesman, D. R. Turner, G. B. Deacon and S. R. Batten, *Chem. Commun.*, 2010, **46**, 4899; (b) Y. Cui, Y. Yue, G. Qian and B. Chen, *Chem. Rev.*, 2012, **112**, 1126; (c) Z.-J. Lin, X. Lin and R. Cao, *Acta Chim. Sinica*, 2012, **70**, 2012; (d) H. J. Cheng, M. Yu, H. X. Li, C. N. Lu, D. X. Li, M. M. Chen, Z. G. Ren and J. P. Lang, *J. Coord. Chem.*, 2013, **66**, 2335; (e) J. Heine and K. Muller-Buschbaum, *Chem. Soc. Rev.*, 2013, **42**, 9232.

5 T. Yamada, K. Otsubo, R. Makiura and H. Kitagawa, *Chem. Soc. Rev.*, 2013, **42**, 6655.

6 M. Eddaoudi, D. B. Moler, H. Li, B. Chen, T. M. Reineke, M. O'Keeffe and O. M. Yaghi, *Acc. Chem. Res.*, 2001, **34**, 319.

7 (a) Z.-J. Lin, L.-W. Han, D.-S. Wu, Y.-B. Huang and R. Cao, Cryst. Growth Des., 2013, **13**, 255; (b) S.-J. Liu, Y. Huang, Z.-J. Lin, X.-F. Li and R. Cao, RSC Adv., 2013, **3**, 9279; (c) M.-L. Ma, C. Ji and S.-Q.Zang, Dalton Trans., 2013, **42**, 10579.

8 (a) Z.-J. Lin, Z. Yang, T.-F. Liu, Y.-B. Huang and R. Cao, *Inorg. Chem.*, 2012, **51**, 1813; (b) H. Y. He, H. Q. Ma, D. Sun, L. L. Zhang, R. M. Wang and D. F. Sun, *Cryst. Growth Des.*, 2013, **13**, 3154; (c) Y. He, H. Furukawa, C. Wu, M. O'Keeffe and B. Chen, *CrystEngComm*, 2013, **15**, 9328; (d) Y.-S. Xue, L. Zhou, M.-P. Liu, S.-M. Liu, Y. Xu, H.-B. Du and X.-Z. You, *CrystEngComm*, 2013, **15**, 6229.

9 K. Binnemans, *Chem. Rev.*, 2009, **109**, 4283.

10 Q. Tang, S. Liu, Y. Liu, D. He, J. Miao, X. Wang, Y. Ji and Z. Zheng, *Inorg. Chem.*, 2013, **53**, 289.

11 (a) Z.-J. Lin, B. Xu, T.-F. Liu, M.-N. Cao, J. Lü and R. Cao, *Eur. J. Inorg. Chem.*, 2010, 3842; (b) Z. Guo, H. Xu, S. Su, J. Cai, S. Dang, S. Xiang, G. Qian, H. Zhang, M. O'Keeffe and B. Chen, *Chem. Commun.*, 2011, **47**, 5551; (c) D. Yan and Q. Duan, *Inorg. Chem. Commun.*, 2013, **36**, 188.

12 J. C. de Mello, H. F. Wittmann and R. H. Friend, *Adv. Mater.*, 1997, **9**, 230.

13 G. M. Sheldrick SHELXS-97, Progam for Crystal Structure Solution and Refinement; University of Göttingen: Göttingen, Germany, 1997.

14 A. L. Spek, *J. Appl. Crystallogr.*, 2003, **36**, 7.

15 (a) R. M. P. Colodrero, K. E. Papathanasiou, N. Stavgianoudaki, P. Olivera-Pastor, E. R. Losilla, M. A. G. Aranda, L. Leon-Reina, J. Sanz, I. Sobrados, D. Choquesillo-Lazarte, J. M. Garcia-Ruiz, P. Atienzar, F. Rey, K. D. Demadis and A. Cabeza, *Chem. Mater.*, 2012, **24**, 3780; (b) G. F. Hou, H. X. Li, W. Z. Li, P. F. Yan, X. H. Su and G. M. Li, *Cryst. Growth Des.*, 2013, **13**, 3374. (c) S. Mishra, E. Jeanneau, A. L. Bulin, G. Ledoux, B. Jouguet, D. Amans, A. Belsky, S. Daniele and C. Dujardin, *Dalton Trans*, 2013, **42**, 12633.

16 (a) D. L. Ma, V. P. Y. Ma, D. S. H. Chan, K. H. Leung, H. Z. He and C. H. Leung, *Coord. Chem. Rev.*, 2012, **256**, 3087; (b) Y. S. Liu, D. T. Tu, H. M. Zhu and X. Y. Chen, *Chem. Soc. Rev.*, 2013, **42**, 6924.

17 (a) V. Chandrasekhar, J. Goura and A. Duthie, *Inorg. Chem.*, 2013, **52**, 4819; (b) I. H. Hwang, H. Y. Kim, M. M. Lee, Y. J. Na, J. H. Kim, H.

C. Kim, C. Kim, S. Huh, Y. Kim and S. J. Kim, *Cryst. Growth Des.*, 2013, **13**, 4815.

18 (a) Y. Luo, Y. J. Zheng, G. Calvez, S. Freslon, K. Bernot, C. Daiguebonne, T. Roisnel and O. Guillou, *CrystEngComm*, 2013, **15**, 706; (b) P. R. Matthes, J. Nitsch, A. Kuzmanoski, C. Feldmann, A. Steffen, T. B. Marder and K. Muller-Buschbaum, *Chem.-Eur. J.*, 2013, **19**, 17369; (c) T. Liu, W. Zhang, W. Sun and R. Cao, *Inorg. Chem.*, 2011, **50**, 5242.

19 R. Decadt, K. Van Hecke, D. Depla, K. Leus, D. Weinberger, I. Van Driessche, P. Van der Voort and R. Van Deun, *Inorg. Chem.*, 2012, **51**, 11623.